Technical Paper

ISSN 1997-1400 Int. J. Pavement Res. Technol. 6(1):8-14

Mixed Mode Fracture Toughness of Recycled Tire Rubber-Filled Concrete for Airfield Rigid Pavements

Muhammad Mubaraki[1+], Amr A. Abd-Elhady[1,2], and Hossam El-Din M. Sallam[1,3]

Abstract: The effect of specimen thickness and crack length on the variations of mode I and mode II stress intensity factors (SIFs) have been analyzed by using three dimensional finite element analysis (3D FEA). Center cracked circular disc specimen (CCCD) was used in this investigation. Eight values of specimen thickness to specimen radius ratio were studied numerically, varied from 0.1 to 0.8. The present experimental research has been conducted to study the effect of replacing 10% of fine aggregate by volume with crumb rubber on crack initiation angle, crack path and fracture toughness for different mode of mixity.

It can be concluded that, the site of crack initiation in notched CCCD specimen was found numerically and experimentally as at the point of the longest vertical coordinate on the notch surface for different inclination notch angle. The value of normalized mode I SIF increased at the mid plane of specimen by increasing the thickness of the specimen. However, at the specimen surface this value decreased by increasing the specimen thickness. For all mode of mixity, the plane stress fracture toughness (G_C) has not been affected by replacing 10% of sand by the rubber particles.

***Key words**: Centre cracked circular disc specimen; Crack growth path; Crack initiation angle; Mixed mode I/II.*

Introduction

Crumb rubber is a material produced by shredding and commutating used tires. The huge stockpile of used tires in the world has been posing an environmental and health hazard to the public. Finding a way to dispose of the rubber in concrete would enhance the understanding on how to incorporate the crumb rubber in greater engineering usage. Other construction products are based on rubber powder obtained from the cryogenic milling of tires, mixed with asphalt or bituminous materials. Recycled tire rubber-filled concrete (RRFC) has become a matter of interest in the last few decades, due to its good performance and as an alternative for tire recycling. This type of concrete provides a good mechanical behavior under static and dynamic actions and is being used for road pavement applications [1-3]. Hernández-Olivares [3,4] studied the static and dynamic mechanical behavior of RRFC from crumb used tires. They found that, the optimum crumb rubber fiber content for the compatibility and stability of cement – rubber interface was 5%. The concrete with this optimum value had a better damping capacity without a significant variation of the concrete mechanical features, either maximum stresses or elastic modulus. Furthermore, they [3] suggested a powerful design tool for rigid pavements design of road construction based Westergaard equations for flat plates on elastic foundations. Their results of RRFC showed the feasibility of using this cement based composite material as a rigid pavement for roads on elastic subgrade.

In practice the pre-existing cracks in the structures are often subjected to complex loading. For such cases, due to arbitrary orientation of flaws relative to the overall applied loads, cracks are subjected to a combination of two major modes of loading: mode I and mode II (mixed mode I/II). The prediction of cracking direction and subsequent crack path is well-recognized problem. Recently, considerable research efforts have been to investigate crack growth behavior under mixed mode I/II loading. A variety of mechanics-based theories have been proposed and used by investigators to predict the direction of crack growth under mixed mode I/II loading [5, 6]. Aliha *et al*. [6] studied the mixed mode I/II crack growth behavior of Guiting limestone by using a semi-circular bend specimen. They observed that, trajectories crack is not only depending on the mode mixity but also on the specimen shape. Disc-type specimens are simple in geometry and have many advantages in terms of specimen preparation, testing and analysis. A Center Cracked Circular disc (CCCD) specimen under diametrical compression and semicircular Specimens under three point bending were used for Mode-II and mixed Mode I-II fracture toughness calculation [7].

Research Significance

The objective of this paper is to study experimentally and numerically the mixed mode fracture behavior in recycled tire rubber-filled concrete. The effect of inclination angle of edge U-notch on the crack initiation and growth behavior was analyzed. The variation of mode I and mode II stress intensity factor through the crack thickness are described.

Numerical Work

CCCD of radius (R) containing a pre-crack of length ($2a$) under uniaxial compressive loading, as shown in Fig. 1, was numerically simulated using 3D finite element analysis for this study. The ratio

[1] College of Engineering, Jazan University, Jazan 706, Kingdom of Saudi Arabia.
[2] On sabbatical leave from Faculty of Engineering, Helwan University, Cairo, Egypt.
[3] On sabbatical leave from Faculty of Eng., Zagazig University, Zagazig, Egypt.
[+] Corresponding Author: E-mail mmubaraki@jazanu.edu.sa
Note: Submitted April 14, 2012; Revised August 13, 2012; Accepted September 3, 2012.

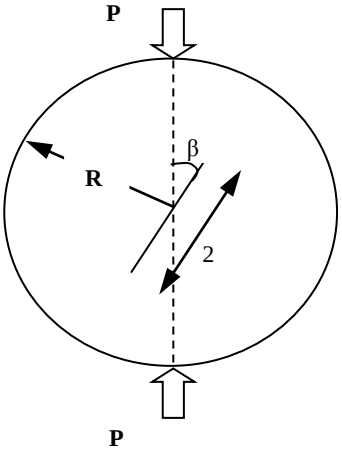

Fig. 1. Center Cracked Circular Disc Specimen.

Table 1. Sieve Analyses of Rubber Particles.

Sieve Opening, mm	5	2.36	1.18	0.60	0.30	0.15
Passing %	100	25.6	2.3	1.86	0.7	0.0

Table 2. Physical Properties of crumb Rubber Particles.

Fineness Modulus	Specific Gravity	Unit Weight (t/m^3)
4.6	1.18	0.472

Table 3. Mix Proportions.

Cement (kg/m³)	Water (kg/m³)	Sand (kg/m³)	Coarse Aggregate (kg/m³)	w/c Ratio
388	186	786	1024	0.48

Table 4. Experimental Values of Compressive, Tensile, and Shear Strength.

Type of Concrete	PC	RuC
Compressive Strength, f_{cu}, MPa	26.6	25
Tensile Strength, MPa	2.34	2.4
Shear Strength, MPa	4.1	4.5
f_{cu} / f_{cu},PC	1	0.94
Tensile/Compression	0.088	0.096
Shear/ Compression	0.154	0.18

of *a/R* was kept constant equal to 0.3. To studying the effect of the specimen thickness, eight values of specimen thickness, 2*t*, to specimen radius ratio, *2t/R*, were considered. The pre-crack makes an angle, *β*, relative to the loading (vertical) direction. Mode mixity parameter of the elastic far field, M^e, was introduced by Shih [8]:

$$M^e = \frac{2}{\pi} arctan\left(\frac{K_I}{K_{II}}\right) \quad (1)$$

where: K_I and K_{II} are mode I and mode II stress intensity factor, respectively.

The values of M^e varied through 1 (pure mode I), 0.75, 0.5, 0.25 and 0 for pure mode II. This mixity parameter was valid for CCCD specimen by change the pre-crack inclination angle, *β*, as 0, 5, 10.5, 18 and 27°. In the present analysis, the mode I and mode II normalized stress intensity factors are denoted as Y_I and Y_{II}, respectively, and it can be deduced from Ref. [7] the general formula for normalized stress intensity factor Y_i, which is defined as:

$$Y_i = \frac{2t\ R\ K_i}{P}\sqrt{\frac{\pi}{a}} \qquad i = I, II \quad (2)$$

where: 2*t* and *R* are the specimen thickness and radius, respectively, *P* is the applied load, and *a* is the crack length.

Several researches assumed the behavior of heterogeneous brittle materials as homogeneous, isotropic and elastic [9-11]. Hammouda *et al*. [9, 10] found that, the kink angle did not depend on the linearity of the material, *i.e.* the material behaves as elastic or elastic-plastic. Therefore, it was assumed that the CCCD specimen materials behave as homogeneous, isotropic and elastic material. The plane *x-y* (plane *z* = 0) is the mid plane of specimen and two specimen surface are *z* = *t* and *z* = -*t*, respectively. ABAQUS (code version 6.9) was used [12] with X-FEM. A 3D finite element model has been developed to account for geometric and material behavior of CCCD material specimen. The finite element meshes constructed with hexagonal structural mesh, C3D8R (8-node linear brick) elements, are used under Standard/static analysis. The thickness of the specimen is divided into 10 planar layers. Within each layer, the size of element decreases gradually with distance from the pre-crack tip decreasing. This means that the finite element (FE) meshes in the neighborhood of the pre-crack tip are much denser. The ABAQUS code was used for numerical calculation of K_I and K_{II} for the CCCD specimen.

Experimental Work

Type I Portland cement was used. The sand used was local natural siliceous sand with a specific gravity of 2.55 and a fineness modulus of 2.52, the coarse aggregate was dolomite with a nominal maximum size of 14 mm and a specific gravity of 2.65. Rubber particles passed through sieve number 4.75 mm and the retained on sieve number 0.15 mm were used as a fine aggregate. Sieve analysis of the rubber particles shown in Table 1.The physical properties of waste rubber are given in Table 2. The normal concrete mix proportions are shown in Table 3. 10% of sand volume was replaced by rubber particles.

The mechanical properties were tested on cubes of 150 x 150 x 150 mm for compression test, cylinders of 150 mm diameter and 300 mm height for indirect tension test, and L-shape 0f 150 x 150 x 260 mm for shear test.

Table 4 shows the experimental results of the compressive, tensile and shear strength of plain concrete (PC) and rubberized concrete (RuC). The decreasing of compressive strength values due to replacing 10% of sand by the rubber particles could be considered negligible. The tensile and shear strength values of RuC are greater than those of PC. The table shows also that the ratios between the tensile and compressive strength are 8.8% and 9.6% and the ratios between shear and compressive strength are 15.4% and 18% for PC and RuC respectively.

Mixed mode fracture toughness was tested on CCCD of 150 mm diameter and 60 mm thickness as show in Fig 1, with notch

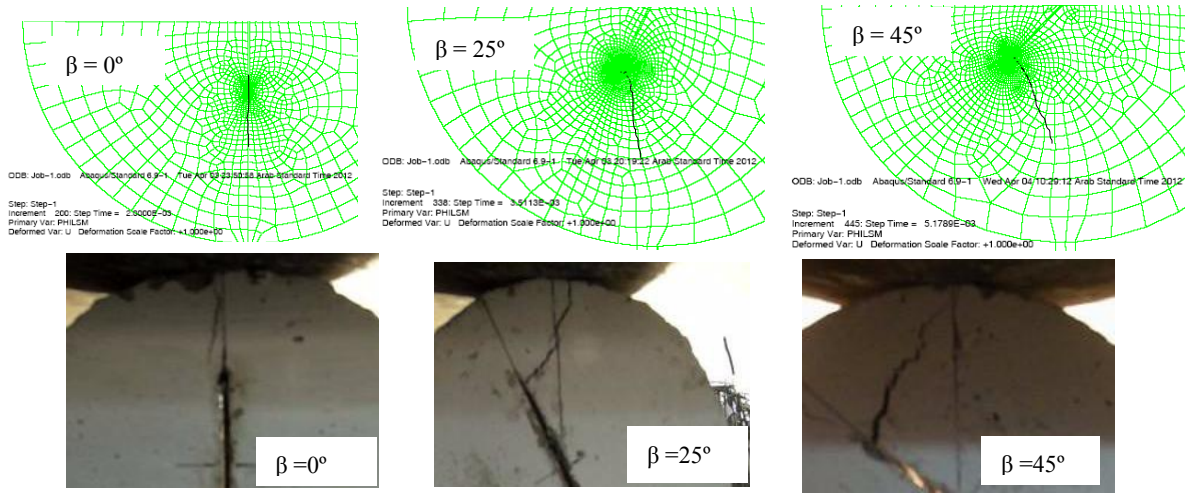

Fig. 2. Site of Crack Initiation.

inclination angle β equals (0, 5, 10, 15, 20, 25, 30, 35, 40, 45, 50, 55^o). Pure mode I fracture toughness exists at β = 0^o, while, pure mode II fracture toughness exists at approximately β = 25^o. The ratios of notch depth, 2*a*, to disc diameter, 2*R*, *i.e. 2a/2R*, are 0.3, 0.4, and 0.5. Five specimens were used for each case of Plain concrete (PC) and Rubberized Concrete (RuC). Stress intensity factor is calculated using the following relationship [13]:

$$K_I = -\frac{P}{2tR}\sqrt{\frac{a}{\pi}}\left\{\begin{array}{l} 2A_0 + \lambda^2(3A_0 + A_2) + \lambda^4\left(\frac{3}{4}A_2 + \frac{3}{4}A_4\right) + \\ \lambda^6\left(\frac{3}{2}A_0 - \frac{1}{2}A_2 + \frac{3}{8}A_4 + \frac{5}{8}A_6\right) \\ + \lambda^8\left(\frac{3}{32}A_0 + \frac{11}{16}A_2 - \frac{3}{32}A_4 + \frac{15}{16}A_6 + \frac{35}{64}A_8\right) \end{array}\right\} \quad (3)$$

$$K_{II} = -\frac{P}{tR}\sqrt{\frac{a}{\pi}}\left\{\begin{array}{l} B_0 - \lambda^2(B_0 + \frac{1}{2}B_2) + \lambda^4(-\frac{1}{8}B_0 + \frac{1}{4}B_2 + \frac{3}{8}B_4) \\ + \lambda^6\ (B_0 - \frac{1}{16}B_2 + \frac{1}{8}B_4 + \frac{5}{16}B_6) + \\ \lambda^8(-\frac{17}{64}B_0 + \frac{3}{8}B_2 - \frac{5}{128}B_4 + \frac{5}{64}B_6 + \frac{35}{128}B_8) \end{array}\right\} \quad (4)$$

where:

A_0 = 0.5 - cos 2β B_0 = sin 2β

A_2=2[-cos 4β+ cos 2β] B_2=2[sin4β -sin2β]

A_4=3[-cos 6β+ cos 4β] B_4=3 [sin6β -2sin4β]

A_6=4[-cos 8β+ cos 6β] B_6=4[sin8β -3sin6β]

A_8=5[-cos 10β+ cos 8β] B_8=5[sin10β -4sin8β]

where *R* and 2*t* are the radius and thickness of the specimen respectively, λ= *a/R*, and β: the notch inclination angle [13].

Hussain *et al*. [14] based the G-criterion on the assumption that the crack under combined loading moved along its own initial plane, and assumed that the combined energy release rate, G, was given by Eq. (5).

$$G = \frac{1}{E`}(K_I^2 + K_{II}^2) \quad (5)$$

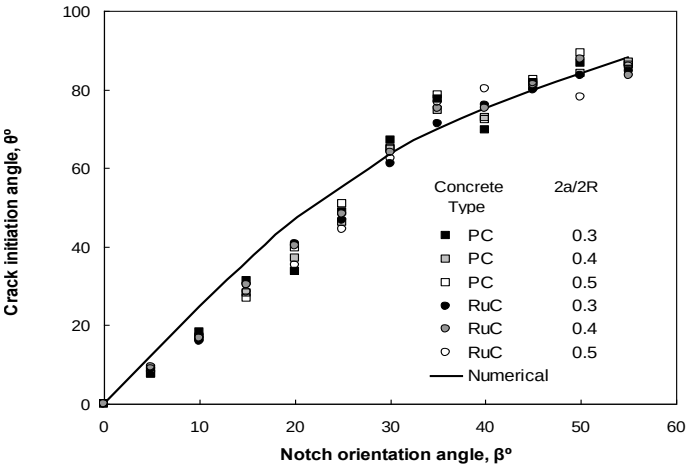

Fig. 3. Crack Initiation Angle (β).

As known, the mode I fracture toughness can be expressed by G_{IC}, $K_{IC} = \sqrt{(G_{IC}E')}$. Where $E' = E$ for the plane stress state and $E' = E'(1 - \nu^2)$ in plane strain state, *E* is the modulus of elasticity of the material and ν is Poisson's ratio. According to ACI code, $E = 4700\sqrt{(fc')}$ MPa, where fc' = cylinder compressive strength, $E \approx 21$ GPa.

Results and Discussion

Crack Initiation Angle and the Crack Growth Trajectory

Crack initiation includes two components: site of crack initiation (location) and crack initiation angle (direction). The site of crack intonation was found at the point of the longest vertical coordinate on the notch rim for different inclination notch angle, see Fig. 2. This is in agreement with numerical results recent obtained by Sallam and Abd-Elhady [5]. On the other hand Aliha *et al*. [6] stated that "Fracture initiated in all samples from the crack tip", but, this is only true for pure mode I. Furthermore, Fig. 2 in their paper [6] support our observation and against their statement.

To predict the crack growth path under mixed mode conditions it is necessary to determine the fracture initiation angle at the crack

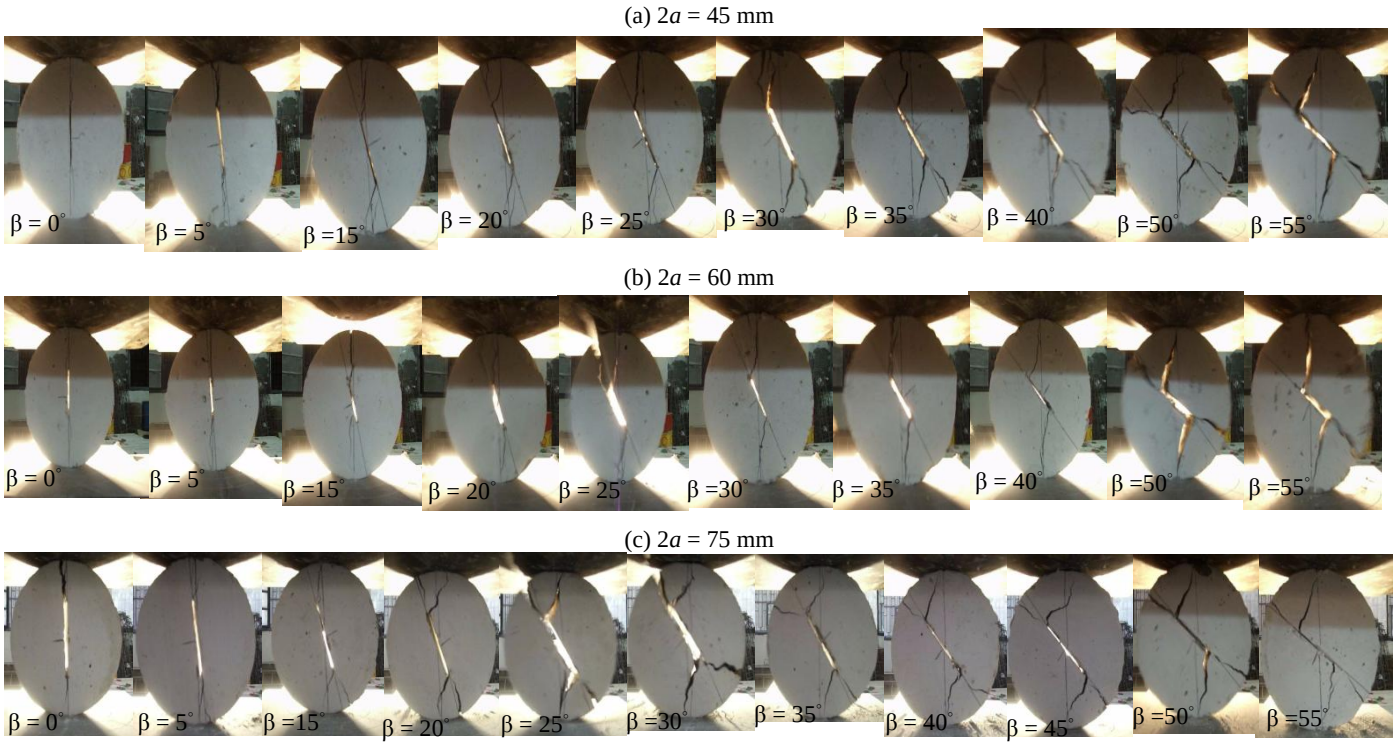

Fig. 4. Failure Modes of PC for (a) 2*a* = 45 mm, (b) 2*a* = 60 mm, and (c) 2*a* = 75 mm.

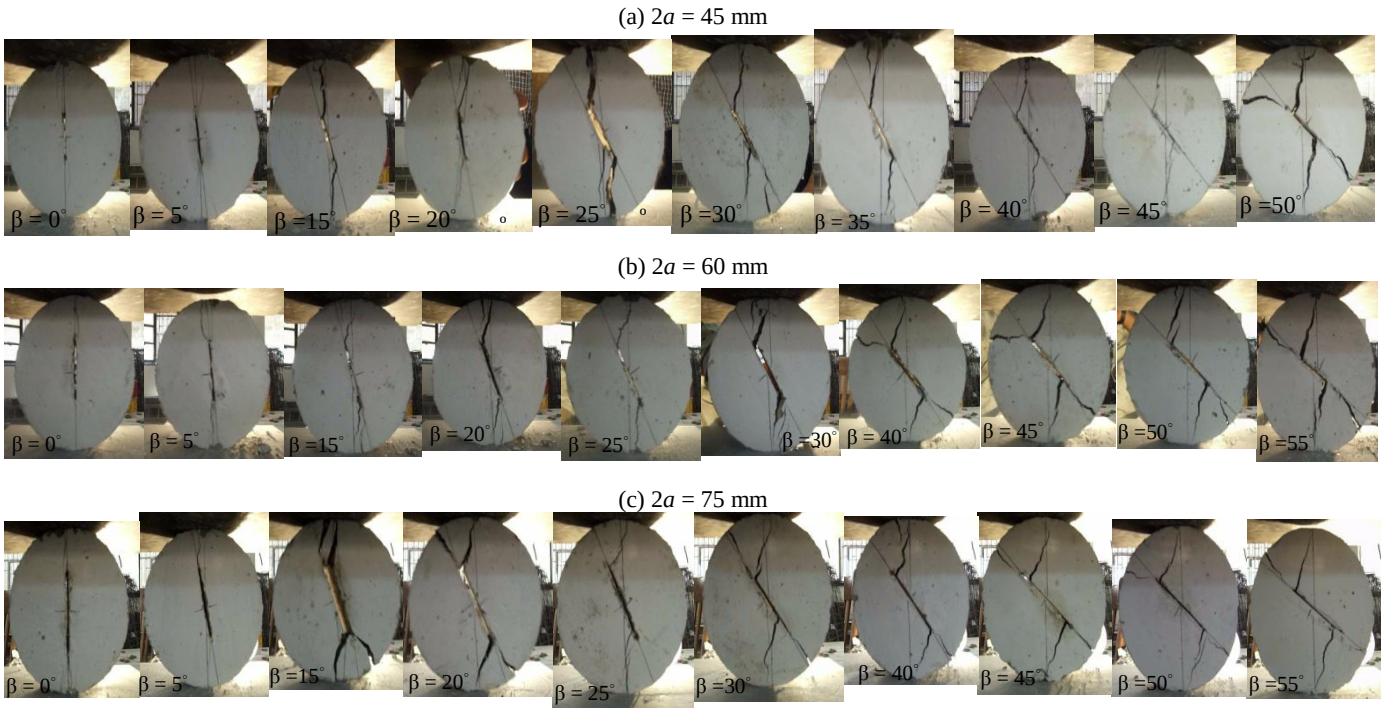

Fig. 5. Failure modes of RuC for (a) 2*a* = 45 mm, (b) 2*a* = 60 mm, and (c) 2*a* = 75 mm.

tip. A number of mixed mode fracture theories have been proposed for determining the direction of brittle fracture. The experimental and the numerical crack initiation angle (θ) versus crack orientation angle (β) is plotted in Fig. 3 for PC and RuC. There is an Agreement between the present experimental results and the predicted values by finite element analysis. There is no clear effect of crack length or 10% rubber replacement on the value of crack initiation angle for different mode of mixity.

The notch remained open during the diametrical compression loading, until the load increases beyond a certain value, at which the cracks initiated and propagated very rapidly along a curvilinear path towards the points on the boundary of the disk where the compression load were applied. Notch remained open during the growth of the crack until reach the boundary of the specimen. When

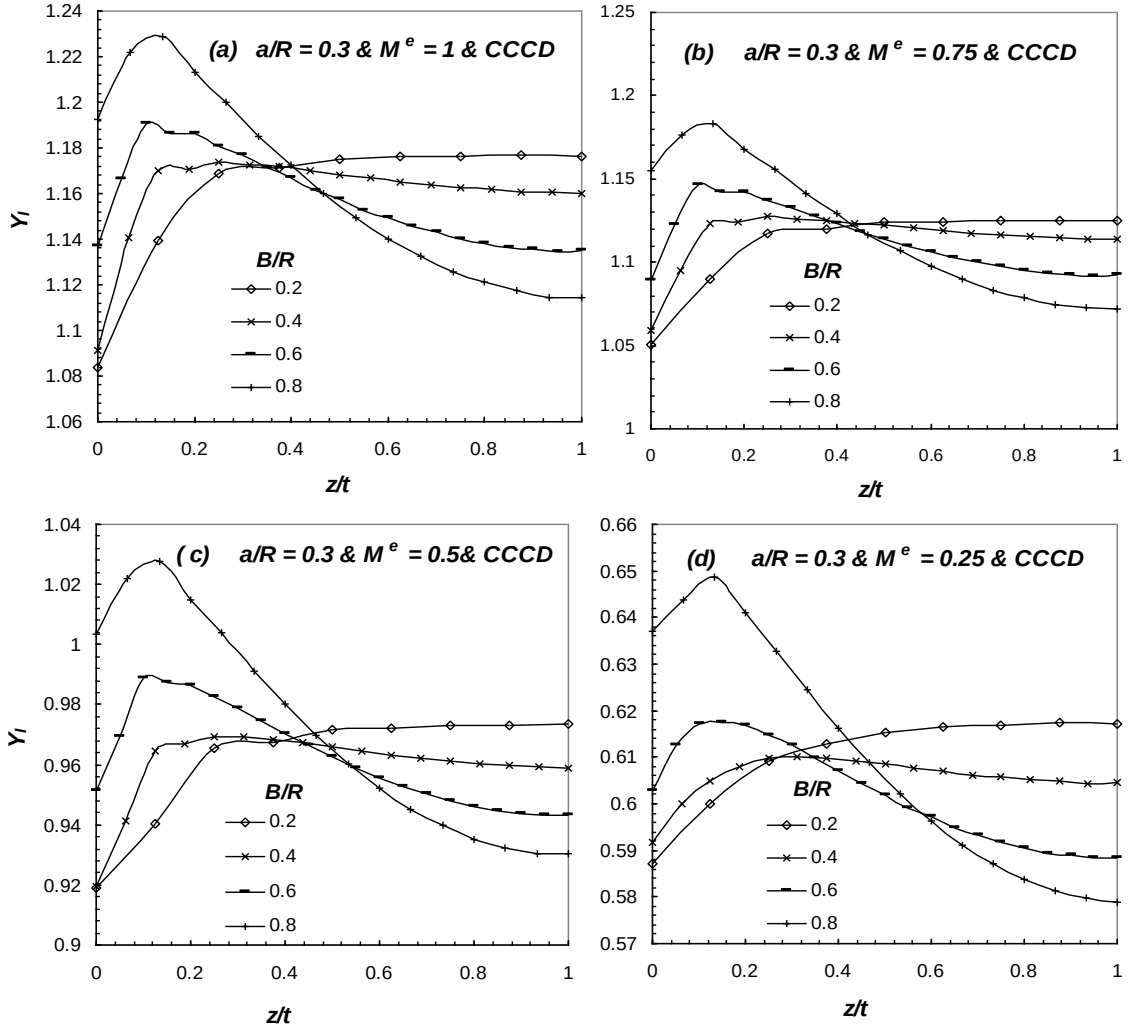

Fig. 6. The Distribution of the Normalized Mode I Stress Intensity Factor Along Crack Front of CCCD Specimen for Different *t* and Different Mode Mixity (a) M^e = 1, (b) M^e = 0.75, (c) M^e = 0.5 and (d) M^e = 0.25.

the propagating crack reached either the upper or the lower boundary of a sample, the sample failed and broke into two pieces, as shown in Fig. 4 and 5. This is in agreement with Aliha *et al*. [6]. The observed fracture patterns for CCCD specimens reveal that the fracture initiation angles and fracture paths were not the same for mixed mode I/II loading. It can be seen in these figures that except for pure mode I conditions (β=0º) which has a fracture path along the initial crack line, the fracture paths were not the same for any other states of mixed mode I/II loading. As is already known, the crack usually growth in the direction perpendicular to the maximum tensile stress, *i.e.* mode I crack growth. At a certain value of β, *i.e.* at a certain value of K_{II}/K_I, beyond it the crack may be branched as shown in Figs. 4 and 5. Crack branching may be attributed to sliding crack extension in the direction of maximum shear stress taking place prior to the final mode I crack growth. This is in agreement with several researches found in the literature in different materials and case of loadings [15-17].

Variation of Y_I and Y_{II} through the Specimen Thickness

Fig. 6 shows the effect of specimen thickness of CCCD specimen on Y_I for different M^e. The value of Y_I increase gradually from the mid plane of the specimen to reach their peak value Y_{Imax}, then decreased gradually to reach the surface of the specimen. This trend is observed for all *B/R* accept *B/R* = 0.2, where, Y_I did not reach the maximum value, *i.e.* the highest value was found at the specimen surface. The value of Y_I increased at the mid plane of specimen, *z/t* = 0, *yy* increasing the thickness of the specimen. However, at the specimen surface, *z/t* = 1, the value of Y_I decreased by increasing the specimen thickness. These trends for all specimen thickness are not dependent on M^e. For thickness ratio, *B/R*, larger than 0.2, the site of peak value of the Y_I is closed to the mid plane but the minimum value of Y_{Imin} located at free surface of the specimen.

Fig. 7 shows the effect of CCCD specimen thickness on the normalized mode II stress intensity factor for different mode mixity and at different position on the crack front *z/t*, *i.e. z/t* = 1, 0.5, 0. For all mode of mixity, there is no significant effect of the specimen thickness on the value of normalized mode II SIF, Y_{II}. versus the CCCD specimen thickness ratio, *B/R*.

Fracture Toughness

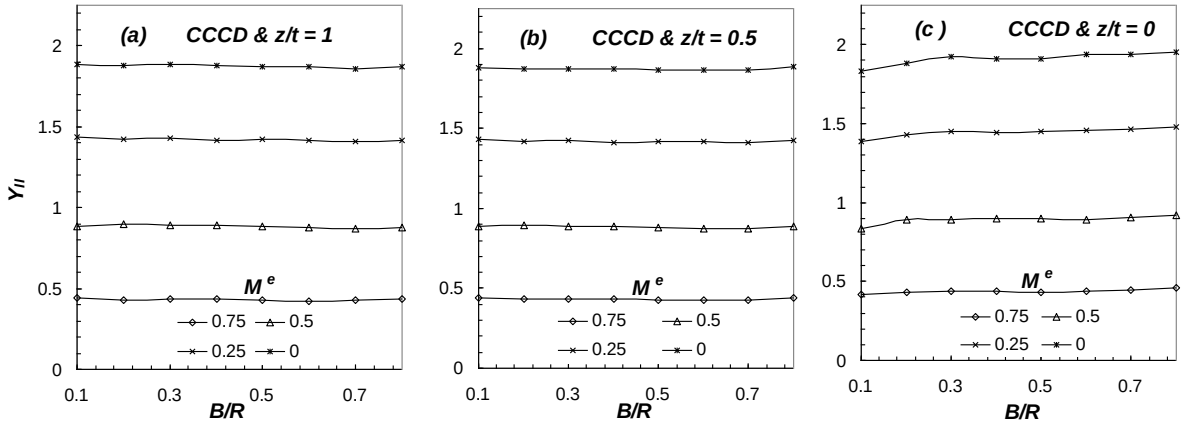

Fig. 7. The Effect of CCCD Specimen Thickness on the Normalized Mode II Stress Intensity Factor for Different Mode Mixity and at Different Position on the Crack Front *z/t*, (a) *z/t* = 1, (b) *z/t* = 0.5, (c) *z/t* = 0.

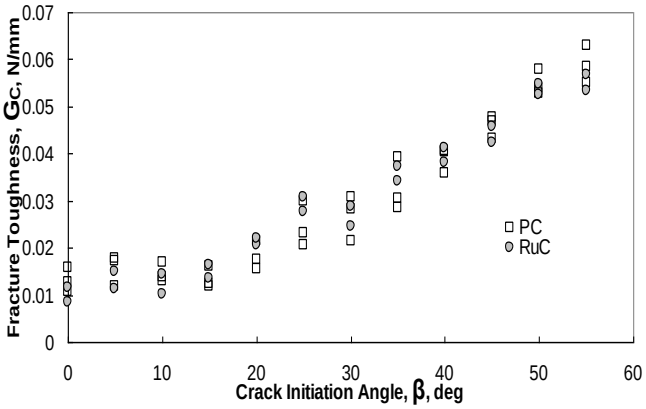

Fig. 8. The Relation between the Fracture Toughness and the Crack Initiation Angle.

Fig. 8 shows the relation between the plane stress fracture toughness (G_C) and the crack initiation angle (β). Its clear that, the fracture toughness increased by increasing β for both concrete types. For all mode of mixity, G_C did not affect by replacing 10% of sand by the rubber particles. In many cases, the reduction in the strength of concrete is limited. However, the results of many other cases showed that the addition of coarse rubber aggregates decreased the strength of concrete markedly [18,19], *i.e.* negative impact on the property of the concrete. On the other hand, the addition of rubber aggregates to concrete improves its dynamic properties [18,20]. Therefore, these studies are worth to make them.

The main advantage of this relation is assist the designer to get accurate solution for concrete pavement design based on fracture mechanics. In general, fracture instability occurs when the strain energy release rate, G, remains larger than the crack resistance, R. A basic concept of arresting crack growth involves the reduction of the effective stresses around the crack tip. Several methods, e.g. reduction of stress concentration, reinforcement of cracked parts, application of residual compressive stresses, etc., are considered to reduce the effective stresses around the crack tip [21, 22]. Concrete pavement design continues to evolve, especially in the types of inputs and slab stresses considered and the ability to accumulate fatigue damage in small-time increments [23]. Ramsamooj *et al.* [24] proposed a new method based on The combination of the theory of elasticity and fracture mechanics called EFM. They compared the results from EFM for the deflection and bending stress at the mid-slab position along the longitudinal edge of a rigid pavement with the experimental data from the AASHO road test. They found that, a good agreement between the results determined by EFM and the test data from the AASHO road test. Recently, Gaedicke et al [23] proposed and employed a fracture mechanics approach to simulate the progressive crack growth and peak load capacity of 3-D concrete slabs on ground and experimentally verified.

Conclusions

Based on the present numerical results, some conclusions were drawn as follows:

1. The site of crack initiation in notched CCCD specimen was found numerically and experimentally as at the point of the longest vertical coordinate on the notch surface for different inclination notch angle.
2. There is an Agreement between the present experimental results of crack initiation angle and that predicted by finite element analysis.
3. At a certain value of β, i.e. at a certain value of KII/KI, beyond it the crack may be branched.
4. The value of normalized mode I SIF increased at the mid plane of specimen by increasing the thickness of the specimen. However, at the specimen surface this value decreased by increasing the specimen thickness.
5. For all mode of mixity, the fracture toughness did not affect by replacing 10% of sand by the rubber particles.

References

1. Zeiada, W., Souliman, M., Stempihar, J., Biligiri1, K.P., Kaloush, K., Said, S., and Hakim, H. (2012). Fatigue Resistance and Crack Propagation Evaluation of a Rubber-Modified Gap Graded Mixture in Sweden, *7th RILEM International Conference on Cracking in Pavements*, Delft,

Netherlands, June 20 – 22 (Accepted).
2. Kaloush, K., Way, G., and Zhu, H. (2005). Properties of Crumb Rubber Concrete, *Transportation Research Record*, No. 1914, pp. 8-14.
3. Hernández-Olivares, F., Barluenga, G., Parga-Landa, B., Bollati, M., and Witoszek, B. (2007). Fatigue Behaviour of Recycled Tyre Rubber-Filled Concrete and Its Implications in the Design of Rigid Pavements, *Construction and Building Materials*, No. 21, pp. 1918–1927.
4. Hernández-Olivares, F., Barluenga, G., Bollati, M., and Witoszek, B. (2002). Static and dynamic Behaviour of Recycled Tyre Rubber-Filled Concrete, *Cement and Concrete Research*, No. 32, pp. 1587–1596.
5. Sallam, H.E.M. and Abd-Elhady, A.A. (2012). Mixed Mode Crack Initiation and Growth in Notched Semi-Circular Specimens-Three Dimensional Finite Element Analysis, *Asian Journal of Materials Science*, 4(2), pp. 34-44.
6. Aliha, M.R.M., Ayatollahi, M.R., Smith, D.J., and Pavier, M.J. (2010). Geometry and Size Effects on Fracture Trajectory in a Limestone Rock under Mixed Mode Loading, Engineering Fracture Mechanics, No. 77, pp. 2200–2212.
7. Atkinson, C., Smelser, R.E., and Sanchez, J. (1982). Combined Mode Fracture via the Cracked Brazilian Disk, *International Journal of Fracture*, No. 18, pp. 279-291.
8. Shih, C.F. (1974). Small-Scale Yielding Analysis of Mixed Mode Plane Strain Crack Problem, *ASTM STP*, No. 560, pp. 187-210.
9. Hammouda, M.M.I., Fayed, A.S., and Sallam, H.E.M. (2003). Stress Intensity Factors of a Shortly Kinked Slant Central Crack with Frictional Surfaces in Uniaxially Loaded Plates, *International Journal of Fatigue*, 25(4), pp. 283-298.
10. Hammouda, M.M.I., Fayed, A.S., and Sallam, H.E.M. (2003). Simulation of Mixed Mode I/II Cyclic Deformation at the Tip of a Short Kinked Inclined Crack with Frictional Surfaces, *International Journal of Fatigue*, 25(8), pp. 743-753.
11. Liu, F., Chen, G., Li, L., and Guo, Y. (2012). Study of Impact Performance of Rubber Reinforced Concrete, *Construction and Building Materials*, No. 36, pp. 604–616.
12. ABAQUS user's manual version 6.9 (2002). Hibbitt, Karlsson and Sorensen Inc., Pawtucket, Rhode Island, USA.
13. Yarema, S.Y., Ivanitskaya, G.S., Maistrenko, A.L., and Zboromirskii, A.I. (1984). Crack Development in a Sintered Carbide in Combined Deformation of Types I and II, *Problemy Prochnosti*, No. 8, pp. 51-56.
14. Hussain, M.A., Pu, S.L., and Underwood, J. (1974). Strain Energy Release Rate for a Crack Under Combined Mode I and Mode II, *Fracture analysis*, ASTM STP, No. 560, pp. 2-28.
15. Gálvez, J.C., Červenka, J., Cendón, D.A., and Saouma, V. (2002). A Discrete Crack Approach to Normal/Shear Cracking of Concrete, *Cement and Concrete Research*, No. 32, pp. 1567–1585.
16. Doquet, V. and Bertolino, G. (2008). Local Approach to Fatigue Cracks Bifurcation, *International Journal of Fatigue*, No. 30, pp. 942–950.
17. Hallbäck, N. (1997). Mixed Mode I/II Fracture Behaviour of a High Strength Steel, *International Journal of Fracture*, No. 87, pp. 363–388.
18. Atahan, A.O. and Yücel, A.Ö. (2012). Crumb Rubber in Concrete: Static and Dynamic Evaluation, *Construction and Building Materials*, No. 36, pp. 617–622.
19. Ozbay, E., Lachemi, M., and Sevim, U.K. (2011). Compressive Strength, Abrasion Resistance and Energy Absorption Capacity of Rubberized Concretes with and without Slag, *Materials and Structures*, No. 44, pp. 1297–1307.
20. Sallam, H.E.M., Sherbini, A.S., Seleem, M.H., and Balaha, M.M. (2008). Impact Resistance of Rubberized Concrete, *Engineering Research Journal*, Minoufiya University, No. 31, pp. 265–271.
21. Sallam, H.E.M., Saba, A.M., Shaheen, H.H., and Abdel-Raouf, H. (2004). Prevention of Peeling Failure in Plated Beams, Journal of Advanced Concrete Technology, *Journal of Advanced Concrete Technology*, Japan Concrete Institute, 2(3), pp. 419-429.
22. Sallam, H.E.M. (1999). A Finite Element Analysis of Fatigue Crack Arresters in Steel Structures, *International Conference of Engineering against Fracture*, University of Sheffield, March 16-21, 1997, UK, Engineering Against Fatigue, Edited by J.H. Beynon, M.W. Brown, R. Smith, T. Lindley, and B. Tomkins, A.A. Balkema Publ., pp. 415-421, 1999.
23. Gaedicke, C., Roesler, J., and Evangelista Jr., F. (2012). Three-Dimensional Cohesive Crack Model Prediction of the Flexural Capacity of Concrete Slabs on Soil, *Engineering Fracture Mechanics* (In Press).
24. Ramsamooj, D.V., Lin, G.S., and Ramadan, J. (1998). Stresses at Joints and Cracks in Highway and Stresses at Joints and Cracks in Highway and Airport Pavements Airport Pavements, *Engineering Fracture Mechanics*, No. 60, pp. 507-518.